Timing-dependent plasticity in human primary somatosensory cortex

Alexander Wolters[1], Arne Schmidt[1], Axel Schramm[2], Daniel Zeller[2], Markus Naumann[2], Erwin Kunesch[1], Reiner Benecke[1], Karlheinz Reiners[2] and Joseph Classen[1,2]

[1]*Human Cortical Physiology Laboratory, Department of Neurology, University of Rostock, D-18147 Rostock, Germany*
[2]*Human Cortical Physiology and Motor Control Laboratory, Department of Neurology, University of Würzburg, D-97080 Würzburg, Germany*

Animal experiments suggest that cortical sensory representations may be remodelled as a consequence of changing synaptic efficacy by timing-dependent associative neuronal activity. Here we describe a timing-based associative form of plasticity in human somatosensory cortex. Paired associative stimulation (PAS) was performed by combining repetitive median nerve stimulation with transcranial magnetic stimulation (TMS) over the contralateral post-central region. PAS increased exclusively the amplitude of the P25 component of the median nerve-evoked somatosensory-evoked potential (MN-SSEP), which is probably generated in the superficial cortical layers of area 3b. SSEP components reflecting neuronal activity in deeper cortical layers (N20 component) or subcortical regions (P14 component) remained constant. PAS-induced enhancement of P25 amplitude displayed topographical specificity both for the recording (MN-SSEP *versus* tibial nerve-SSEP) and the stimulation (magnetic stimulation targeting somatosensory *versus* motor cortex) arrangements. Modulation of P25 amplitude was confined to a narrow range of interstimulus intervals (ISIs) between the MN pulse and the TMS pulse, and the sign of the modulation changed with ISIs differing by only 15 ms. The function describing the ISI dependence of PAS effects on somatosensory cortex resembled one previously observed in motor cortex, shifted by ∼7 ms. The findings suggest a simple model of modulation of excitability in human primary somatosensory cortex, possibly by mechanisms related to the spike-timing-dependent plasticity of neuronal synapses located in upper cortical layers.

(Received 10 February 2005; accepted after revision 18 April 2005; first published online 21 April 2005)
Corresponding author J. Classen: Human Cortical Physiology and Motor Control Laboratory, Department of Neurology, Bayerische Julius-Maximilians Universität, Josef-Schneider Str. 11, 97080 Würzburg, Germany. Email: classen_j@klinik.uni-wuerzburg.de

Understanding the rules that shape human central sensory representations is of considerable physiological and clinical interest. Lasting changes of synaptic efficacy, long-term potentiation (LTP) and long-term depression (LTD), have been implicated as physiological mechanisms underlying experience- and injury-driven sensory map changes in humans and animals (Merzenich *et al.* 1983; Pons *et al.* 1991). Indeed, LTP/LTD have been documented in the somatosensory cortex of experimental animals using a variety of induction protocols both *in vitro* (Aroniadou-Anderjaska & Keller, 1995; Castro-Alamancos *et al.* 1995; Castro-Alamancos & Connors, 1996; Kitagawa *et al.* 1997; Feldman, 2000; Heusler *et al.* 2000; Urban *et al.* 2002) and *in vivo* (Keller *et al.* 1990; Glazewski *et al.* 1998; Froc *et al.* 2000; Allen *et al.* 2003; Werk & Chapman, 2003). These protocols differ substantially with respect to their efficacy and physiological properties (for review see Buonomano & Merzenich, 1998; Fox, 2002). Among the protocols, spike-timing-dependent plasticity of synaptic efficacy (STDP; Song *et al.* 2000) is unique in that the direction of synaptic efficacy changes is determined by the sequence of pre- and postsynaptic neuronal activity (for review see Dan & Poo, 2004). In STDP, LTP is induced if the postsynaptic neurone fires an action potential after the excitatory postsynaptic potential is induced by the presynaptic neurone. In contrast, LTD is generated if the sequence of events is reversed. STDP is largely independent of the neuronal firing rate and possesses significant theoretical advantages over models of plasticity that are solely driven by average correlations between the firing of different neurones (Sejnowski, 1999; Song *et al.* 2000; Song & Abbott, 2001). In humans, the plasticity of sensory representations has been studied in a variety of clinical and behavioural conditions by the analysis of somatosensory-evoked potentials (SSEPs)

 DOI: 10.1113/jphysiol.2005.084954

(Elbert *et al.* 1995; Flor *et al.* 1995, 1997; Knecht *et al.* 1996; Tinazzi *et al.* 1997*b*, 1998, 2004; Bara-Jimenez *et al.* 1998; Elbert *et al.* 1998). Different components of SSEPs reflect different stages of somatosensory information processing (Tinazzi *et al.* 1998). Therefore, the analysis of SSEPs enables the site of plastic changes along the neuroaxis to be located (Tinazzi *et al.* 1998). SSEPs have also been used to probe excitability changes induced experimentally by various external manipulations such as direct current stimulation (Matsunaga *et al.* 2004), repetitive transcranial magnetic stimulation (Enomoto *et al.* 2001; Tsuji & Rothwell, 2002; Ragert *et al.* 2004), or repetitive peripheral tactile stimulation (Pleger *et al.* 2001). However, it is not possible, using these protocols, to test for the presence of plasticity mechanisms that exhibit properties of STDP in human primary somatosensory cortex (S1). Recently, we have introduced paired associative stimulation (PAS) in humans as a protocol shaped after animal models of associative LTP/LTD. PAS consists of pairing repetitive peripheral electrical afferent stimulation with transcranial magnetic stimulation (TMS) of the primary motor cortex (Stefan *et al.* 2000, 2002; Wolters *et al.* 2003). In this arrangement, transcranial magnetic stimulation probably activates intracortical fibres travelling 'horizontally' with respect to the cortical surface (Rothwell, 1997), and peripheral electrical stimulation induces activity in cortico-petal (thalamo-cortical or cortico-cortical) 'vertical' fibres (Kaas & Pons, 1988). Unlike other plasticity-inducing protocols, PAS allows the control of the relative timing of neuronal events induced by the two stimulation modalities. PAS targeting the primary motor cortex (M1) induces either potentiation or depression of TMS-evoked potentials (Wolters *et al.* 2003) depending on the interval between the two stimulation modalities, and the physiological properties of this plasticity resemble those of STDP seen in animal studies (Stefan *et al.* 2000, 2002; Wolters *et al.* 2003).

Here, we use PAS with TMS over the somatosensory cortex to test the hypothesis that a timing-dependent plasticity rule governs the induction of bidirectional plasticity in human S1. Together, our findings provide further support for the notion that timing-dependent plasticity may represent an important principle subserving neocortical plasticity in humans.

Methods

Subjects

The protocol conformed to the principles of the *Declaration of Helsinki* and was approved by the ethics committees of the Universities of Rostock and Würzburg. Experiments were performed on 64 healthy volunteers (31 men, 33 women), aged 20–48 years (mean 26.7 ± 6.0 years) with normal results on neurological examination. All subjects gave their written informed consent to the procedures.

Stimulation

Electrical nerve stimulation was performed with a Grass stimulator (Type S88, Grass Instruments, West Warwick, Richmond, VA, USA) connected to a stimulus isolation unit (SIU 8T, Grass Instruments) or with an electrical stimulator (Digitimer D7AH, Digitimer, Welwyn Garden City, UK) with a standard stimulation block (cathode proximal). Transcranial magnetic stimulation (TMS) was performed using a flat figure-of-eight-shaped magnetic coil (diameter of each wing: 70 mm) connected to a Magstim 200 magnetic stimulator (Magstim, Whitland, Dyfed, UK). The coil was held tangentially to the skull with the handle pointing backwards and laterally at an angle of 45 deg to the sagittal plane.

Recording

Electroencephalographic (EEG) signals were recorded from the scalp using needle electrodes (model 9013R0312, Medtronic, Skovlunde, Denmark) or Hwato acupuncture needles (Suzhou Medical Appliance Factory, Suzhou, China) in a bipolar montage with the reference electrode placed frontocentrally at Fz according to the international 10/20 system (Klem *et al.* 1999). To ensure that the same EEG recording positions were used before and after PAS, electrodes remained at the recording sites during the interventional stimulation. During PAS, EEG recording electrodes were disconnected from the amplifier. Although the pressure of the coil on the underlying electrode caused slight discomfort this was well tolerated by all subjects. Surface electromyographic (EMG) activity was recorded from the right abductor pollicis brevis muscle (APB) using disposable Ag–AgCl surface electrodes (Neuroline model 725 01-SC, Medicotest, Olstykke, Denmark, or reusable Ag–AgCl electrodes (Fischer Medizintechnik, Nürnberg, Germany) with the active electrode mounted on the muscle belly and the inactive electrode placed over the base of the metacarpo-phalangeal joint of the thumb. EEG and EMG signals were amplified (model BF/IEC 601-1, Jaeger-Toennies, Freiburg, Germany, or 1902 amplifier, Cambridge Electronics Design, Cambridge, UK). EEG signals were bandpass filtered between 0.2 and 1500 Hz, and EMG signals between 5 and 2000 Hz. Data were sampled at 5000 Hz using an A/D converter (model 1401 plus, Cambridge Electronics Design) and stored in a laboratory computer for display and later offline analysis.

Experimental procedures

The principal purpose of all experiments was to determine the effect of a paired associative stimulation protocol on SSEPs recorded from the scalp positions overlying S1.

Subjects were seated in a comfortable reclining chair. The optimal position of the magnetic coil for eliciting

motor-evoked potentials (MEPs) in the right APB was assessed over the left motor cortex at a moderately suprathreshold stimulation intensity, and marked directly on the scalp with a soft-tip pen. At the optimal site, termed 'motor hot spot', the resting motor threshold (RMT) was determined as the stimulator intensity needed to produce a response of at least 50 μV in the relaxed APB in at least 5 of 10 consecutive trials at a resolution of 1% of the maximal stimulator output (Rossini *et al.* 1994). Throughout the experiment, complete muscle relaxation was monitored by audio-visual feedback.

Somatosensory-evoked potentials (SSEPs). For MN-SSEPs, EEG signals were recorded in a bipolar montage with the active electrode placed at C3′ and the reference electrode at Fz according to the international 10/20 system (Mauguiere *et al.* 1999). The C3′ position was determined 2 cm posterior to the C3 position (Nuwer *et al.* 1994). Median nerve stimulation was performed using a pulse width of 300 μs (Grass stimulator) or 200 μs (Digitimer D7AH) at a frequency of 3 Hz and a stimulation intensity of 300% of the individual perceptual threshold. For each sweep the recorded time interval extended from 30 ms before to 70 ms (MN-SSEP) or 120 ms (TN-SSEP), respectively, after the stimulus artifact. An SSEP represented the average of 250 responses. For TN-SSEP, the active electrode was placed over Cz′ and the reference electrode over Fz (Mauguiere *et al.* 1999). In all experiments, four SSEPs were obtained each before, and immediately after the intervention (see below). Sweeps were rejected automatically online if the signal following the stimulus artefact exceeded a limit of $\pm$ 20 μV. Furthermore, individual sweeps containing artifactual signals were eliminated after offline visual analysis.

Paired associative stimulation (PAS). The PAS intervention represented a modification of a protocol published previously by our group (Stefan *et al.* 2000; Wolters *et al.* 2003). In a typical experiment, repetitive single electrical stimuli were delivered to the right median nerve at the level of the wrist at 300% of the perceptual threshold (10.4 ± 1.7 mA), each followed by TMS delivered over a position 2 cm posterior to the 'motor hot spot'. Previous results (Okamoto *et al.* 2004) as well as unpublished observations from our laboratory (A. Schramm & D. Zeller) using a neuronavigation system revealed that this position overlies the postcentral gyrus. This position was found to correspond closely to C3′. TMS was applied at an intensity of 1.5 times the resting motor threshold ($SI_{1.5RMT}$). Taking all experiments into consideration, $SI_{1.5RMT}$ amounted to 51 ± 9% of the maximal stimulator output. The interval between MN stimulation and the subsequent TMS pulse was set at the individual N20 latency. N20 latency was defined as the mean latency of the N20 component of all four baseline SSEPs. One hundred and eighty pairs were delivered at 0.1 Hz over 30 min.

After PAS, four additional MN-SSEPs were obtained. Identical stimulation parameters were used before and after intervention. The principal experimental design shared by all experiments is illustrated in Fig. 1. Variations of the experimental standard protocol are described below.

Care was taken that subjects maintained a steady level of attention to the task during the SSEP recordings and during the PAS intervention.

Duration and reversibility

In 10 subjects modulation of MN-SSEPs following the intervention (PAS_{N20}) was monitored over time. Four MN-SSEPs were obtained each immediately (0 min), and at 30, 60 and 90 min after PAS.

Topographical specificity of PAS_{N20} effects

Comparison of PAS_{N20} effects on MN-SSEP and TN-SSEP. In nine subjects, the effect of PAS_{N20} on MN-SSEP was compared with that on the SSEP elicited by stimulation of the right tibial nerve (TN-SSEP) in the same experimental session. The sequence of MN-SSEP and TN-SSEP prior to and post intervention was counterbalanced throughout this experimental condition.

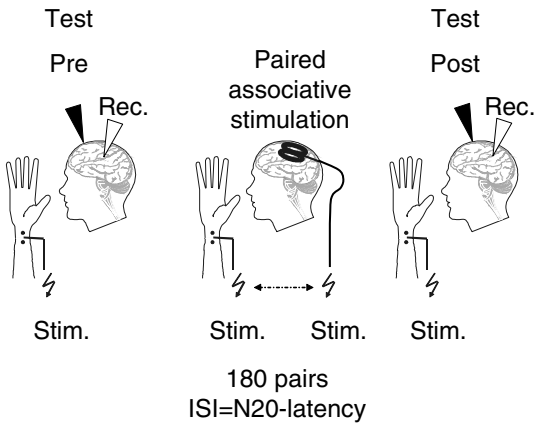

Figure 1. Principles of experimental design
Test somatosensory-evoked potentials (SSEPs) were elicited by right median nerve stimulation (MN-SSEPs) before and after the intervention. During paired associative stimulation 180 pairs were delivered, each consisting of electrical stimulation of the right median nerve followed by TMS delivered through a magnetic coil placed over the left hemisphere 2 cm posterior to the optimal site for activating the abductor pollicis brevis (APB) muscle. In the principal experiment, the interstimulus interval was set at the N20 latency of the MN-SSEP as determined before paired associative stimulation (PAS). An inter-pair interval of 10 s was used (0.1 Hz). Rec., recording site of SSEP. Open arrowhead, active electrode; filled arrowhead, reference electrode. Stim., peripheral nerve stimulation or transcranial magnetic cortex stimulation.

Effect of PAS employing ulnar nerve stimulation on ulnar nerve-evoked somatosensory potentials (UN-SSEP). In a separate series on six subjects, PAS_{N20} was performed by afferent stimulation of the ulnar nerve and delivering TMS at a skull site located 2 cm posterior to the 'motor hot spot' of the abductor digiti minimi muscle.

Effect of varying the site of magnetic stimulation. In eight subjects the effect of PAS_{N20} intervention performed with the magnetic coil positioned over the postcentral gyrus was compared with PAS_{N20} intervention performed with the magnetic coil positioned over the 'motor hot spot' of the APB muscle which corresponds to M1 (Classen *et al.* 1998). The sequence of these two experimental conditions was counterbalanced and sessions were separated by at least 2 days.

Effect of varying the interval between median nerve stimulation and TMS

The timing of the TMS pulse with reference to the median nerve stimulation was varied. Ten different ISIs were tested in a total of 104 separate experimental sessions on 62 different subjects. ISI was set at N20 latency + x with x as $-40, -30, -20, -10, -5, -2.5, 0, +5, +10, +20$ ms. These interventions were termed $PAS_{N20-40ms}$, $PAS_{N20-30ms}$, ... $PAS_{N20+20ms}$, respectively. A minimum number of five experiments were performed for each ISI. In cases where subjects participated in more than one experiment, at least 2 days elapsed between any two sessions.

Data analysis

SSEPs were analysed offline. Baseline was determined as the average value over a period of 30 ms immediately before the stimulus (Regan, 1989). In several initial experiments blinded assessment of baseline was shown to be virtually identical with non-blinded assessment. The N20 amplitude was assessed as the difference between the baseline and the first negative peak occurring at a latency of around 17–21 ms after the time of median nerve stimulation, and the amplitude of the N20–P25 complex was determined as the difference between the N20 peak and the subsequent positivity. Subsequently, P25 amplitude was calculated as the difference between the amplitude of the N20–P25 complex and the N20 amplitude. In some experiments the P14 amplitude was additionally assessed from baseline to peak. The P14 component could not be reliably identified in all subjects. Therefore, all PAS_{N20} experiments were randomly screened for the presence of a reliable P14 component until 15 consecutive experiments displaying a P14 component were identified. The latency of the N20 component in MN-SSEP was determined at the maximum negativity. The P40 component of the TN-SSEP is thought to be equivalent to the P25 component of the MN-SSEP (Yamada *et al.* 1996; Yamada, 2000). The P40 peak was identified at latencies of 34–46 ms and its amplitude was determined as the difference from baseline.

For each subject, the values of each parameter were averaged across the four SSEP repetitions and the means were entered into the final statistical analyses.

For display purposes, averages of four SSEPs ('grand average') (sets of 4 SSEPs collected at individual time points before and after intervention) were generated for individual subjects. Similarly, averages of grand averages ('great grand averages') were computed to illustrate group results. Great grand averages were obtained after prior alignment of grand averages to the individual N20 latency.

Data were analysed using Student's t tests and analyses of variance (ANOVA). In general, two-tailed t tests were employed. If an *a priori* hypothesis on the sign of the tested difference could be made, one-tailed t tests were used. Details of the ANOVA factors tested are given in Results. Effects were considered significant if $P < 0.05$.

Modelling

Modelling of the function relating the PAS-induced magnitude of P25 amplitude change to the interval between the stimulation modalities was done using commercially available software (DataFit program, Version 8.0, Oakdale Engineering, Oakdale, PA, USA).

The following function was found empirically

$$y = a + \frac{x/b - c}{(x/b - c)^4 + d} \quad (1)$$

Initial parameter estimates were determined graphically. Variance analysis was used to test the overall significance of the regression model. The null hypothesis H_0 ($a = b = c = d = 0$) was tested against the hypothesis H_1 (($a \neq 0$) or ($b \neq 0$) or ($c \neq 0$) or ($d \neq 0$): at least one parameter is different from 0). In a variation of the regression model ('model 2', parameter 'a' set to $a = 1$), the null hypothesis H_0 ($b = c = d = 0$) was tested against H_1 (($b \neq 0$) or ($c \neq 0$) or ($d \neq 0$)).

If not stated otherwise, all group data are given as mean ± S.D.

Results

Principal experiment

TMS over the somatosensory cortex was timed to coincide with the individual N20 latency of the MN stimulation-evoked potential. Following PAS_{N20}, MN-SSEP was changed (Fig. 2*A*). All experimental sessions considered (a total of 40 experimental sessions on 35 volunteers), PAS_{N20} led to an increase of the N20–P25 amplitude from a mean of $5.6 \pm 2.9\,\mu V$ to

$6.0 \pm 3.1\ \mu$V ($P = 0.001$, paired two-tailed t test; Fig. 2*B*), or, on average, by 6.2%. Inspection of the raw data revealed that MN-SSEP tracings started to separate from the tracings recorded before intervention at about 3 ms after the N20 peak. This observation suggested a differential effect of PAS_{N20} on the N20 and P25 components. Therefore, the amplitude of these components was determined separately. Following PAS_{N20}, the amplitude of the N20 peak remained essentially constant (pre-PAS $2.1 \pm 1.3\ \mu$V to $2.0 \pm 1.1\ \mu$V, $P = 0.270$, paired two-tailed t test; Fig. 2*B*), the change amounting to, on average, –0.6%. In contrast, the amplitude of the P25 component increased from a mean of $3.5 \pm 2.0\ \mu$V to $3.9 \pm 2.2\ \mu$V ($P < 0.001$, paired two-tailed t test; Fig. 2*B*), or, on average, by 11.5%.

To investigate the location of PAS-induced changes, the amplitude of the subcortically generated P14 component was analysed in 15 experiments. Following PAS_{N20}, the baseline-normalized amplitudes of the P14 and P25 differed significantly ($P < 0.001$, paired one-sided t test; Fig. 2*C*). P25 amplitude increased from a mean of $3.6 \pm 2.0\ \mu$V pre-PAS to $4.0 \pm 2.1\ \mu$V post-PAS ($P = 0.001$), or, on average, by 14.1%. In contrast, the amplitude of the P14 component did not change significantly (pre-PAS: $0.4 \pm 0.1\ \mu$V; post-PAS: $0.3 \pm 0.1\ \mu$V; $P = 0.107$; mean percentage change −4.8%).

To exclude the possibility that the increase of P25 amplitude was related to a more efficient peripheral nerve stimulation following PAS_{N20}, median nerve sensory nerve action potentials (SNAPs) were recorded simultaneously with the recording of MN-SSEPs in 10 subjects. Following PAS_{N20}, the baseline-normalized amplitudes of the P25 and SNAP differed significantly ($P = 0.035$, paired one-tailed t test; Fig. 2*D*). P25 amplitude increased from a mean of $4.6 \pm 1.9\ \mu$V pre-PAS to $5.2 \pm 2.1\ \mu$V post-PAS ($P = 0.001$), or, on average, by 14.1%. By contrast, the SNAP amplitude remained essentially constant (pre-PAS: $19.0 \pm 10.5\ \mu$V; post-PAS: $19.9 \pm 13.1\ \mu$V; $P = 0.504$; mean percentage increase, 1.4%).

Duration and reversibility

The magnitude of the P25 amplitude was monitored for 90 min. The PAS_{N20}-induced increase of the mean P25 amplitude lasted at least 30 min. P25 amplitude returned to baseline at 90 min. Repeated measures ANOVA ('Time' (baseline, 0, 30, 60, 90 min)) revealed a significant effect of time ($F_{4,36} = 2.837$; $P = 0.038$). Pre-planned contrasts revealed significant differences between P25 amplitude at

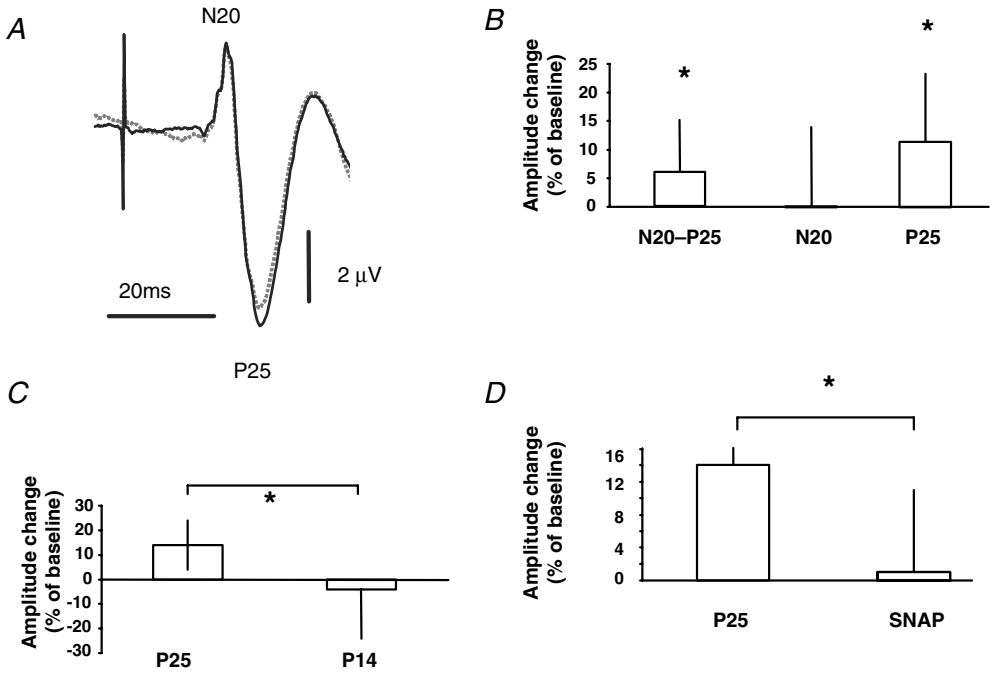

Figure 2. Effect of PAS_{N20} on MN-SSEP
A, example trace of one subject. Average of 4 MN-SSEPs recorded before (grey dotted trace) and after (black trace) intervention with PAS_{N20} (paired associative stimulation with an interval of N20 latency). *B*, group data of 40 experiments on 35 subjects. Percentage change (relative to baseline) of different components of the N20–P25 complex. *C*, comparison of baseline-normalized P25 amplitude (left column) and P14 amplitude (right column). Data from 15 subjects. *D*, comparison of baseline-normalized P25 amplitude (left column) and sensory nerve action potential (right column). Data from 10 subjects. *B–D*, data show mean ± S.D. Asterisks indicate statistical significance.

baseline on the one hand and at 0 min ($P = 0.006$) and 30 min ($P = 0.020$) on the other (paired one-sided t test). P25 amplitude was not significantly different from baseline at 60 and 90 min (Fig. 3).

Topographical specificity of PAS_{N20} effects

To examine the spatial specificity of the effect induced by combined stimulation of MN and TMS over the hand representation in S1, the change of MN-SSEP was compared to that of TN-SSEP which represents the cortical leg representation located at a distance of several centimetres from the hand representation. PAS_{N20} led to a differential effect on MN-SSEP and TN-SSEP (Fig. 4*A*). The baseline-normalized amplitudes of P25 and P40 were significantly different ($P = 0.044$, paired two-sided t test). P25 amplitude increased from a mean of $3.9 \pm 2.1\ \mu$V pre-PAS to $4.2 \pm 2.2\ \mu$V post-PAS ($P = 0.007$, paired one-sided t test), while the P40 amplitude did not change significantly (pre-PAS: $2.7 \pm 0.8\ \mu$V; post-PAS: $2.5 \pm 0.9\ \mu$V; $P = 0.221$). This finding suggests that PAS_{N20}-induced excitability change did not spill over to a remote representation that did not receive spatially homologous information.

To examine whether PAS was able to induce a change in cortical representations that differed from MN-associated regions, PAS was performed with the ulnar nerve as the afferent stimulation route, and the magnetic coil placed over a position located 2 cm posterior to the 'motor hot spot' of the abductor digiti minimi muscle. Following this intervention, the P25 component of the UN-SSEP increased from a mean of $2.6 \pm 0.9\ \mu$V to $2.9 \pm 0.8\ \mu$V ($P = 0.012$), or, on average, by 19.8% (data not illustrated).

To test the possibility that P25 amplitude changes may have been the result of activation of neuronal elements in M1 by current spreading from the site of magnetic stimulation, paired stimulation involving TMS over S1 was compared to paired stimulation involving TMS over M1. Repeated measures ANOVA (2×2, with factors 'Stimulation site' (M1, S1) and 'Time' (pre-PAS, post-PAS)) revealed a significant 'Stimulation site' × 'Time' interaction ($F_{1,7} = 26.636$; $P = 0.001$) suggesting that the effect of PAS_{N20} on MN-SSEP depended on the magnetic coil position during the intervention (Fig. 4*B*). With the magnetic coil positioned over S1, P25 amplitude increased from a mean of $4.2 \pm 1.5\ \mu$V pre-PAS to $5.0 \pm 1.9\ \mu$V post-PAS ($P = 0.005$), or, on average, by 18.6%. In contrast, following PAS with the magnetic coil positioned over M1, the P25 amplitude remained constant (pre-PAS: $4.3 \pm 1.5\ \mu$V; post-PAS: $4.3 \pm 1.6\ \mu$V; $P = 0.969$; mean percentage change −0.3%).

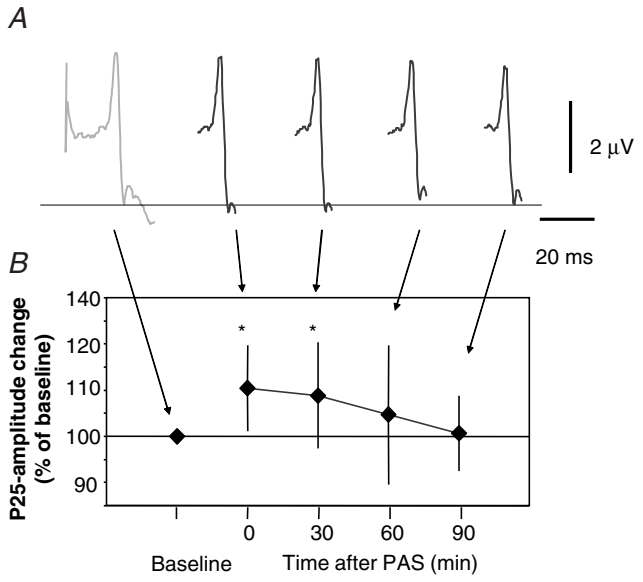

Figure 3. Lasting effect of PAS_{N20}-induced increase of P25 amplitude
A, example trace of one subject. Averages of 4 consecutive MN-SSEPs from the same subject, recorded before PAS_{N20} (grey), and at different times after PAS_{N20} (black). Horizontal line indicates P25 amplitude at baseline. *B*, group data of 10 subjects. Asterisks indicate times when P25 amplitude was significantly ($P < 0.05$) different from baseline. Data show mean ± S.D.

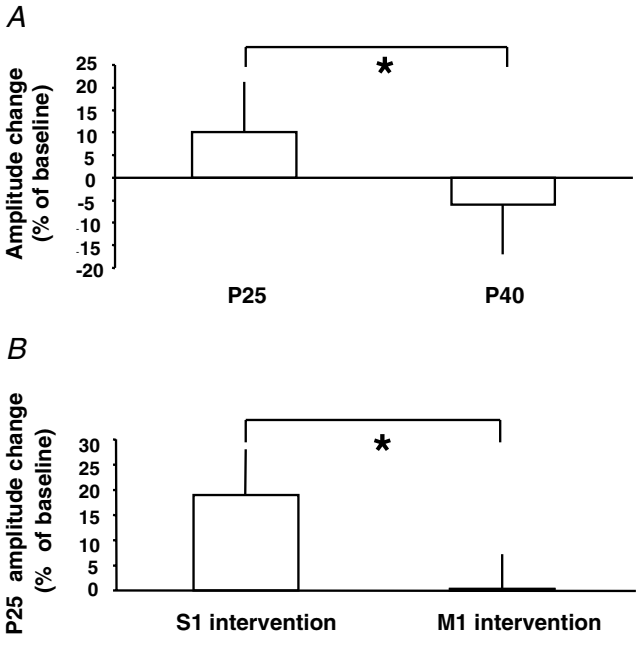

Figure 4. Topographical specificity of PAS_{N20} effects
A, comparison of effects of PAS_{N20} on MN-SSEP and TN-SSEP. PAS_{N20} led to an increase of P25 amplitude (left column) of MN-SSEP while it did not significantly change the amplitude of the P40 amplitude (right column) of TN-SSEP. Data from 9 subjects (mean ± S.D.). *B*, effect of varying the site of magnetic stimulation. PAS_{N20} intervention was done with the magnetic coil placed over S1 (left column) or M1 (right column). Data from 8 subjects (mean ± S.D.). Asterisks indicate statistical significance.

Effect of varying the interval between median nerve stimulation and TMS

To test the hypothesis that MN stimulation paired with TMS at appropriate intervals would lead to bidirectional changes in S1, the interstimulus interval between the median nerve stimulation and the magnetic stimulation over S1 was varied over a wide range of intervals. Repeated measures ANOVA (10×2, between-subject factor 'ISI' ($-40, \ldots 20$), within-subject factor 'Time' (pre-PAS, post-PAS)) revealed a significant interaction term 'ISI' × 'Time' ($F_{9,94} = 5.109$; $P < 0.001$; Fig. 5) suggesting that P25 amplitude change depended on ISI. *Post hoc* testing revealed that P25 amplitude increased with $PAS_{N20-5ms}$ ($P = 0.036$, paired two-tailed *t* test), $PAS_{N20-2.5ms}$ ($P = 0.023$) and PAS_{N20} ($P < 0.001$). P25 amplitude decreased with $PAS_{N20-20ms}$ ($P = 0.007$).

To estimate the timing of the equilibrium between facilitating and depressing effects of PAS on P25 amplitude, data were modelled by fitting parameters of eqn (1) which was found empirically. Initial parameter estimates were determined graphically. The results of two different models with four (model 1) or three (parameter '*a*' set to $a = 1$, model 2) regression variables are displayed in Table 1. Equation (1) generated a fit of the data explaining 91.6% (model 1) or 86.4% (model 2) of the variance. For both models, the time of equilibrium between facilitating and depressing effects of PAS was computed to be N20 latency – 9.2 ms.

In a previous study PAS was used to target M1. The magnitude of PAS-induced changes of the motor-evoked potentials recorded from the abductor pollicis brevis muscle varied as a function of the interval between median nerve stimulation and magnetic stimulation of M1 (Wolters *et al.* 2003). To compare the ISI dependence of PAS targeting M1 (Wolters *et al.* 2003) with those observed in the present study, all ISIs from the previous study were recalibrated to the mean N20 latency of 18.8 ms found in a representative subgroup of subjects (Wolters *et al.* 2003). Data were modelled using eqn (1). The regression variables from the current experiments were used as initial parameter estimates. Equation (1) generated a fit of the data explaining 86.3% (model 1) or 74.3% (model 2) of the variance (Table 1). Using these regression variables the time of equilibrium of facilitating and depressing effects of PAS targeting M1 was computed to be N20 latency – 2.4 ms (model 1) or N20 latency – 2.7 ms (model 2). Therefore, the difference between the times of equilibrium with PAS targeting S1 *versus* PAS targeting M1 was 6.8 ms (model 1, Fig. 6) or 6.5 ms (model 2).

Discussion

The present results have shown that peripheral stimulation of somatosensory afferents, if paired with low-frequency TMS at appropriate intervals, may induce bidirectional changes in somatosensory-evoked potentials.

Regional and laminar location of PAS-induced SSEP changes

Representational plasticity may occur at each anatomical level of the central somatosensory system (Florence & Kaas, 1995; Nicolelis *et al.* 1998; Tinazzi *et al.* 1998;

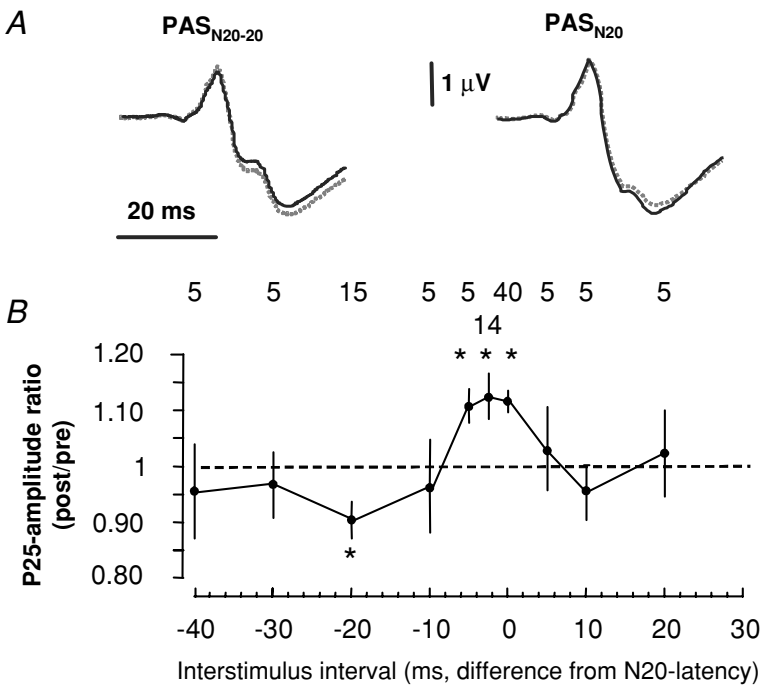

Figure 5. Dependence of PAS-induced effects on the interval between afferent peripheral nerve stimulation and transcranial magnetic stimulation
A, 'great grand' averages (see Methods) for tracings obtained at ISI = N20 latency − 20 ms ($PAS_{N20-20ms}$, left) and ISI = N20 latency (PAS_{N20}, right) (grey dotted trace, before intervention; black trace, after intervention). Great grand averages were generated by aligning SSEPs to the peak of the N20 component. *B*, for each interval 5–35 subjects were tested. Abscissa: intervals relative to the individual N20 latency. Asterisks indicate that changes of P25 amplitude are significantly different from the baseline condition. Number of experiments for each interval shown in top row. Data are mean ± standard error of the mean.

Table 1. Results of modelling SSEP and MEP changes as a function of interstimulus interval between afferent stimulation and TMS

Regression variable	SSEP		MEP	
	Model 1	Model 2	Model 1	Model 2
a	0.981	**1**	1.074	**1**
b	5.270	5.204	8.659	8.278
c	−1.738	−1.770	−0.277	−0.333
d	5.987	7.022	2.072	2.165
R^2	0.874	0.825	0.781	0.658
F ratio	$F_{3,6} = 21.822$	$F_{2,7} = 22.245$	$F_{3,5} = 10.492$	$F_{2,6} = 8.686$
Probability (*P*)	0.001	0.001	0.013	0.017

Four (model 1) or three (model 2) regression variables were used to fit eqn (1) (cf. Methods). In model 2, regression variable *a* was kept constant (bold, $a = 1$). R^2, adjusted coefficient of multiple determination. *F* ratio is shown with degrees of freedom: regression, error.

Jones, 2000; Chung *et al.* 2002). The P14 component of MN-SSEP is known to be generated subcortically, possibly in the terminal part of the ascending lemniscal system at its arrival in the ventroposterior lateral nucleus of the thalamus (Desmedt & Cheron, 1981; Moller *et al.* 1986; Sonoo *et al.* 1997; Lee & Seyal, 1998). Following PAS_{N20}, the amplitude of the P14 component remained unchanged (Fig. 2). Therefore, PAS did not induce SSEP changes arising at a level below the thalamus.

Of the two early cortical SSEP components evaluated, changes were induced in the P25 component, while the amplitude of the N20 component remained constant (Fig. 2*B*). The generators of the early components of the MN-SSEP have been extensively investigated over the past decades (for review see Allison *et al.* 1991) with respect to their regional and laminar origin. Both the N20 and the P25 components are now widely accepted to be generated in the posterior bank of the central sulcus, corresponding to Brodmann area 3b (Allison *et al.* 1989, 1991; McLaughlin & Kelly, 1993; Urbano *et al.* 1997; Lee & Seyal, 1998; Mauguiere *et al.* 1999; Legatt & Kader, 2000; Balzamo *et al.* 2004). Therefore, changes in the P25 component probably indicate excitability changes in S1, although it is possible that a minor contribution to the P25 component arises from the anterior bank of the central sulcus in Brodmann area 4 (Huang *et al.* 2000; Balzamo *et al.* 2004). The issue of an additional contribution to changes in the P25 component by an anterior source in area 4 or by an additional radial source residing in area 1 may be clarified further only by applying multi-dipole localization algorithms to multichannel recordings (Huang *et al.* 2000).

The N20 component of the MN-SSEP is believed to reflect the passive source current for active depolarizing sinks on the cell bodies and proximal apical dendrites of pyramidal cells in layer 4, the input layer of the cortex (Allison *et al.* 1991). Conversely, the P25 component probably reflects the depolarization of the superficial portion of apical dendrites located in cortical layers 2/3 (Mitzdorf, 1985; Vaughan & Arezzo, 1988; Allison *et al.* 1991; McLaughlin & Kelly, 1993; Nicholson Peterson *et al.* 1995). This concept is underlined by electrical recordings

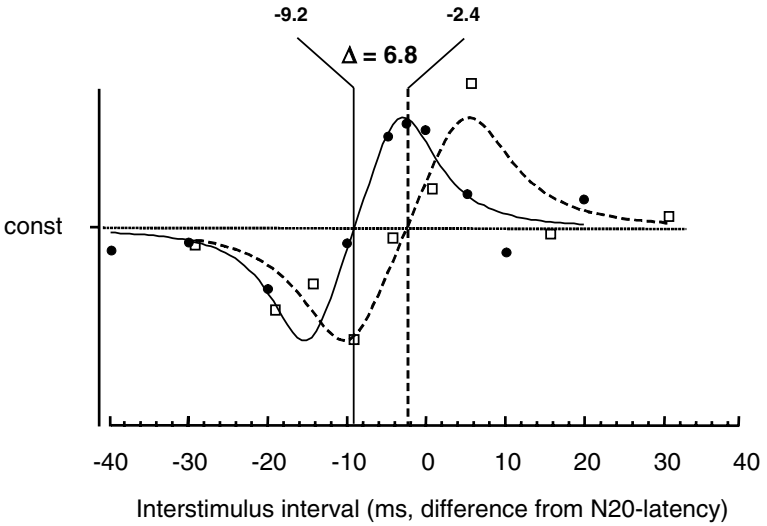

Figure 6. Comparison of ISI dependence of PAS-induced excitability changes in S1 and M1
Fitted data were scaled to their relative extremes. ●, data from the current experimental series. □, data from Wolters *et al.* (2003). S1 curve crosses the level of equilibrium at an ISI shorter by 6.8 ms than the M1 curve.

in animals along the depth of the somatosensory cortex indicating that information is serially relayed from layer 4 to layer 2/3 and that this takes 2–4 ms (Armstrong-James *et al.* 1992; Ahissar *et al.* 2001). This consideration may suggest that PAS-induced cortical excitability changes were due to modulation of excitatory neuronal activity in upper cortical layers of S1. Alternatively, changes of cortical excitability could be due to alterations in (tonic) inhibition impinging on cortical pyramidal cells. As some of this inhibition is under subcortical thalamic control, it is important to consider the possibility that PAS-induced excitability changes may in fact have been generated subcortically, rather than locally within the cortex. Virtually all thalamo-cortical projections to area 3b terminate in layer 4 and lower layer 3 (Jones, 1986). Therefore, given the serial nature of information transmission from layer 4 to layer 2/3, both N20 and P25 components should be similarly affected by changes in thalamo-cortical activity. Hence, the differential modulation of the N20 component and the P25 component renders a subcortical origin of cortical excitability changes unlikely.

Our observation concurs with previous findings that combined peripheral and cortical stimulation may lead to facilitation of subsequently recorded MN-SSEPs (Tsuji & Rothwell, 2002). Just as in the present study, SSEP changes were absent for the subcortical P14 component. Interestingly, inspection of Fig. 2 of the same study suggests selective modulation of P25 amplitude (Tsuji & Rothwell, 2002). These authors used a pairing protocol in which the magnetic coil was placed over M1, a position which was found ineffective (at ISI = N20 latency) in the present study (cf. Fig. 4*B*). One may hypothesize that in their study SSEP changes have been induced in M1 and transmitted to S1 via changes in tonic afferent activity. Alternatively, and more likely, SSEP changes may have been induced in S1 through TMS stimulus spread towards S1. Tsuji & Rothwell (2002) used repetitive motor-point stimulation of the first interosseus muscle, delivered as a pulse train of 500 ms duration, as afferent stimulus. Although only the first of the pulses actually preceded TMS delivered after 25 ms, a train of 10 additional afferent stimuli, following within 500 ms, may have boosted a weak effect that would have been induced in S1 by the pairing of the first pulse with local TMS-evoked effects. Alternatively, comparatively greater activation of muscle spindle afferents may have played a role. More studies are needed to explain this difference between our results and those of Tsuji & Rothwell.

Physiological nature of PAS-induced SSEP changes

The evidence reviewed so far argues for local PAS-induced changes in upper cortical layers of Brodmann area 3b. Possible cellular mechanisms may be inferred by additional physiological properties of these changes. PAS-induced plasticity of the P25 component evolved rapidly (after an intervention of only 30 min), persisted for a considerable length of time (at least 30 min), and was reversible. Topographical specificity of the induced changes was suggested by the fact that MN-SSEPs were altered while TN-SSEPs remained unchanged (although the P40 amplitude in TN-SSEP has been shown to be modifiable by other manipulations; Tinazzi *et al.* 1997*a*). Further, PAS-induced plasticity was distinctly timing dependent. Effects occurred within a narrow window of ISIs. Finally, slightly changing the interstimulus interval between the afferent pulse and the magnetic cortical pulse (from N20 latency – 20 ms to N20 latency − 5 ms) caused the P25 amplitude to change in the opposite direction. This surprising dependence on the timing of PAS-induced plasticity in S1 resembles STDP in animal somatosensory cortex. In a study on cortical slices taken from rat barrel cortex, single excitatory postsynaptic potentials (EPSPs) were paired with single postsynaptic action potentials evoked by current injection through the recording electrode (Feldman, 2000). LTP was observed consistently when the EPSP led the postsynaptic action potential by short (3–15 ms) intervals. In contrast, LTD occurred when the action potential led the EPSP by 0–50 ms. Just 40 pairings were sufficient to induce robust LTP (Feldman, 2000). Together, these physiological similarities may indicate that modulations of synaptic efficacy by mechanisms resembling STDP in animal studies also underlie PAS-induced excitability changes. Interestingly, while LTP/LTD was induced at vertical inputs to layer 2/3 pyramidal cells, layer 4 neurones did not express synaptic plasticity (Feldman, 2000). Therefore, PAS-induced plasticity shares with spike-timing-dependent LTP/LTD in S1 not only its timing properties but possibly also its laminar location in upper cortical layers. Our observations concur with several studies in experimental animals suggesting that synapses in upper cortical layers may have a special role in rapidly induced sensory map plasticity (Diamond *et al.* 1993, 1994; Glazewski & Fox, 1996; Huang *et al.* 1998) while modulation of synaptic plasticity in layer 4, as a rule, is largely restricted to an early developmental period (Fox, 1992) and does not depend on the firing order of pre- and postsynaptic spikes (Egger *et al.* 1999). While the physiological properties of PAS-induced plasticity are suggestive of a synaptic origin, timing-dependent changes of intrinsic neuronal excitability (Daoudal & Debanne, 2003; Zhang & Linden, 2003; Li *et al.* 2004) may represent pre- or postsynaptic mechanisms involved synergistically in generating somatosensory plasticity.

Afferent signals may interact with late TMS-induced cortical neuronal events

For STDP to be operative the postsynaptic neuronal events must follow presynaptic events to induce enhancement

of synaptic efficacy, and the sequence of neuronal events must be reversed for depression. The shortest interval leading to a significant enhancement of P25 amplitude was 5 ms shorter than the individual N20 latency. At this ISI the afferent information had not yet reached the somatosensory cortex. Possibly TMS-induced (post-synaptic) neuronal activity could follow that induced by afferent MN stimulation-induced (presynaptic) activity if a Hebbian interaction between the two events took place subcortically, e.g. in somatosensory thalamus via TMS-activated (Bestmann *et al.* 2004) cortico-thalamic projections. However, as outlined above, this possibility would appear to be inconsistent with the conclusion (based on the differential modulation of N20 amplitude and P25 amplitude) that PAS-induced facilitation of the P25 component had been generated locally, within the cortex.

Indeed, even at ISI = N20 latency − 5 ms, a pre- > postsynaptic sequence of neuronal events would be present in somatosensory cortex if late polysynaptic rather than early direct or monosynaptic TMS-induced activity interacts with presynaptic MN stimulation-induced events. This speculation appears to be well supported by current models of how TMS may activate cortical elements (Amassian *et al.* 1987; Ziemann & Rothwell, 2000). Following a single pulse of TMS to M1, the cortex emits a train of descending action potentials (termed D-waves and I-waves) that may last longer than 10 ms (Di Lazzaro *et al.* 2004). While the early components of this train are thought to be generated in lower cortical layers, the later I-waves probably reflect activity generated in upper motor cortical layers through a chain of inter-neurones (Amassian *et al.* 1987; Ziemann & Rothwell, 2000). We propose that TMS may induce late polysynaptic activity in upper layers of S1 through a similar mechanism to that in M1 and that it is these late events which interact with afferent signals in upper cortical layers of S1. This hypothesis also offers an explanation for the observation, in M1, that PAS effectively increased MEP amplitudes when ISIs between MN stimulation and TMS as short as 20 ms were employed (Ziemann *et al.* 2004). At this interval it is conceivable that late, but not early, TMS-induced events follow those induced by afferent activity in M1. This consideration predicts that late, rather than early, I-waves are modulated by PAS targeting M1.

S1 leads M1 in timing-dependent plasticity

The function describing the dependence of modulation of the P25 amplitude on the exact interstimulus interval between the MN pulse and the TMS pulse closely resembled the function describing the previously established ISI dependence of modulation of the MEP amplitude (Wolters *et al.* 2003). At the ISI indicating equilibrium between enhancing and depressing effects the two curves were shifted by ∼6.8 ms. This observation concurs with studies, both in humans and in non-human primates, suggesting that a somatosensory signal generally arrives in primary motor cortex several milliseconds later than the appearance of the signal in S1 (Goldring *et al.* 1970; Balzamo *et al.* 2004; Gow *et al.* 2004). As there is no direct anatomical connection from area 3b to area 4 (Jones, 1986; Darian-Smith *et al.* 1993) a somatosensory signal from S1 destined for M1 must first be relayed in areas 1 and 2 (Jones, 1986). Although it appears that 6.8 ms may be just sufficient for the travel time along this route, we cannot dismiss the alternative possibility of an afferent pathway to M1 via its private direct thalamic input (Lemon & van der Burg, 1979; Asanuma *et al.* 1980).

Bidirectional timing-dependent plasticity in human S1

In humans, experimental or disease-induced de-afferentation (Tinazzi *et al.* 1997*b*, 1998, 2003) leads to changes in cortical somatosensory representations as assessable by evoked potentials. It may be hypothesized that Hebbian mechanisms such as LTP/LTD may be operative in some of these changes. However, it remains unknown whether STDP of synaptic efficacy is involved. First, it is unclear whether peripheral deafferentation can change the firing behaviour of neurones such that LTP or LTD formation would be promoted. While this question cannot be addressed directly in humans, recent experiments in animals provide strong arguments. In rats, whisker clipping, a model of partial deafferentation, was shown to change the firing order of neurones across different cortical layers (Celikel *et al.* 2004). This study therefore linked deafferentation to neuronal firing patterns that drive spike-timing-dependent LTP/LTD. Secondly, while spike-timing-dependent LTP/LTD has previously been demonstrated *in vitro*, in rats (Feldman, 2000) it was hitherto unknown whether human S1 holds *in vivo* a mechanism for timing-dependent bidirectional modulation of local excitability. Our study, demonstrating STDP-like plasticity in S1, appears to close this gap of information. We propose that it is partly through this mechanism that tactile deafferentation gives rise to lasting changes in human cortical somatosensory representations. Analogous considerations may apply for S1 plasticity induced by tactile coactivation in humans (Pleger *et al.* 2001, 2003), and whisker pairing in rats (Diamond *et al.* 1993). While the available evidence is consistent with involvement of spike-timing-dependent LTP/LTD in naturally occurring somatosensory cortex plasticity, future experiments must address the important question of whether timing-dependent bidirectional modulation of synaptic efficacy in S1 is sufficient to produce bidirectional behavioural changes. Such a relationship was recently suggested in the visual cortex. Pairings of two differently orientated near-synchronous visual stimuli

led to changes of orientation tuning whose direction depended on the temporal order of presentation (Yao & Dan, 2001; Fu *et al.* 2002). Therefore, plasticity driven by timing relationships may represent a general principle of mnemonic representation in neocortex with important behavioural implications. This plasticity may be accessible *in vivo* in different human brain regions ranging from visual (Yao & Dan, 2001; Fu *et al.* 2002) and somatosensory cortex (this study) to motor cortex (Wolters *et al.* 2003) by simple non-invasive stimulation protocols.

In summary, our findings demonstrate that associative stimulation may induce bidirectional excitability changes in human somatosensory cortex. These changes are possibly located in superficial cortical layers and resemble spike-timing-dependent long-term potentiation or depression of neuronal synapses.

References

Ahissar E, Sosnik R, Bagdasarian K & Haidarliu S (2001). Temporal frequency of whisker movement. II. Laminar organization of cortical representations. *J Neurophysiol* **86**, 354–367.

Allen CB, Celikel T & Feldman DE (2003). Long-term depression induced by sensory deprivation during cortical map plasticity in vivo. *Nat Neurosci* **6**, 291–299.

Allison T, McCarthy G, Wood CC & Jones SJ (1991). Potentials evoked in human and monkey cerebral cortex by stimulation of the median nerve. A review of scalp and intracranial recordings. *Brain* **114**, 2465–2503.

Allison T, McCarthy G, Wood CC, Williamson PD & Spencer DD (1989). Human cortical potentials evoked by stimulation of the median nerve. II. Cytoarchitectonic areas generating long-latency activity. *J Neurophysiol* **62**, 711–722.

Amassian VE, Stewart M, Quirk GJ & Rosenthal JL (1987). Physiological basis of motor effects of a transient stimulus to cerebral cortex. *Neurosurgery* **20**, 74–93.

Armstrong-James M, Fox K & Das-Gupta A (1992). Flow of excitation within rat barrel cortex on striking a single vibrissa. *J Neurophysiol* **68**, 1345–1358.

Aroniadou-Anderjaska V & Keller A (1995). LTP in the barrel cortex of adult rats. *Neuroreport* **6**, 2297–2300.

Asanuma H, Larsen K & Yumiya H (1980). Peripheral input pathways to the monkey motor cortex. *Exp Brain Res* **38**, 349–355.

Balzamo E, Marquis P, Chauvel P & Regis J (2004). Short-latency components of evoked potentials to median nerve stimulation recorded by intracerebral electrodes in the human pre- and postcentral areas. *Clin Neurophysiol* **115**, 1616–1623.

Bara-Jimenez W, Catalan MJ, Hallett M & Gerloff C (1998). Abnormal somatosensory homunculus in dystonia of the hand. *Ann Neurol* **44**, 828–831.

Bestmann S, Baudewig J, Siebner HR, Rothwell JC & Frahm J (2004). Functional MRI of the immediate impact of transcranial magnetic stimulation on cortical and subcortical motor circuits. *Eur J Neurosci* **19**, 1950–1962.

Buonomano DV & Merzenich MM (1998). Cortical plasticity: from synapses to maps. *Annu Rev Neurosci* **21**, 149–186.

Castro-Alamancos MA & Connors BW (1996). Short-term synaptic enhancement and long-term potentiation in neocortex. *Proc Natl Acad Sci U S A* **93**, 1335–1339.

Castro-Alamancos MA, Donoghue JP & Connors BW (1995). Different forms of synaptic plasticity in somatosensory and motor areas of the neocortex. *J Neurosci* **15**, 5324–5333.

Celikel T, Szostak VA & Feldman DE (2004). Modulation of spike timing by sensory deprivation during induction of cortical map plasticity. *Nat Neurosci* **7**, 534–541.

Chung S, Li X & Nelson SB (2002). Short-term depression at thalamocortical synapses contributes to rapid adaptation of cortical sensory responses in vivo. *Neuron* **34**, 437–446.

Classen J, Knorr U, Werhahn KJ, Schlaug G, Kunesch E, Cohen LG, Seitz RJ & Benecke R (1998). Multimodal output mapping of human central motor representation on different spatial scales. *J Physiol* **512**, 163–179.

Dan Y & Poo MM (2004). Spike timing-dependent plasticity of neural circuits. *Neuron* **44**, 23–30.

Daoudal G & Debanne D (2003). Long-term plasticity of intrinsic excitability: learning rules and mechanisms. *Learn Mem* **10**, 456–465.

Darian-Smith C, Darian-Smith I, Burman K & Ratcliffe N (1993). Ipsilateral cortical projections to areas 3a, 3b, and 4 in the macaque monkey. *J Comp Neurol* **335**, 200–213.

Desmedt JE & Cheron G (1981). Prevertebral (oesophageal) recording of subcortical somatosensory evoked potentials in man: the spinal P13 component and the dual nature of the spinal generators. *Electroencephalogr Clin Neurophysiol* **52**, 257–275.

Diamond ME, Armstrong-James M & Ebner FF (1993). Experience-dependent plasticity in adult rat barrel cortex. *Proc Natl Acad Sci U S A* **90**, 2082–2086.

Diamond ME, Huang W & Ebner FF (1994). Laminar comparison of somatosensory cortical plasticity. *Science* **265**, 1885–1888.

Di Lazzaro V, Oliviero A, Pilato F, Saturno E, Dileone M, Mazzone P, Insola A, Tonali PA & Rothwell JC (2004). The physiological basis of transcranial motor cortex stimulation in conscious humans. *Clin Neurophysiol* **115**, 255–266.

Egger V, Feldmeyer D & Sakmann B (1999). Coincidence detection and changes of synaptic efficacy in spiny stellate neurons in rat barrel cortex. *Nat Neurosci* **2**, 1098–1105.

Elbert T, Candia V, Altenmuller E, Rau H, Sterr A, Rockstroh B, Pantev C & Taub E (1998). Alteration of digital representations in somatosensory cortex in focal hand dystonia. *Neuroreport* **9**, 3571–3575.

Elbert T, Pantev C, Wienbruch C, Rockstroh B & Taub E (1995). Increased cortical representation of the fingers of the left hand in string players. *Science* **270**, 305–307.

Enomoto H, Ugawa. Y, Hanajima R, Yuasa K, Mochizuki H, Terao Y, Shiio Y, Furubayashi T, Iwata NK & Kanazawa I (2001). Decreased sensory cortical excitability after 1 Hz rTMS over the ipsilateral primary motor cortex. *Clin Neurophysiol* **112**, 2154–2158.

Feldman DE (2000). Timing-based LTP and LTD at vertical inputs to layer II/III pyramidal cells in rat barrel cortex. *Neuron* **27**, 45–56.

Flor H, Braun C, Elbert T & Birbaumer N (1997). Extensive reorganization of primary somatosensory cortex in chronic back pain patients. *Neurosci Lett* **224**, 5–8.

Flor H, Elbert T, Knecht S, Wienbruch C, Pantev C, Birbaumer N, Larbig W & Taub E (1995). Phantom-limb pain as a perceptual correlate of cortical reorganization following arm amputation. *Nature* **375**, 482–484.

Florence SL & Kaas JH (1995). Large-scale reorganization at multiple levels of the somatosensory pathway follows therapeutic amputation of the hand in monkeys. *J Neurosci* **15**, 8083–8095.

Fox K (1992). A critical period for experience-dependent synaptic plasticity in rat barrel cortex. *J Neurosci* **12**, 1826–1838.

Fox K (2002). Anatomical pathways and molecular mechanisms for plasticity in the barrel cortex. *Neuroscience* **111**, 799–814.

Froc DJ, Chapman CA, Trepel C & Racine RJ (2000). Long-term depression and depotentiation in the sensorimotor cortex of the freely moving rat. *J Neurosci* **20**, 438–445.

Fu YX, Djupsund K, Gao H, Hayden B, Shen K & Dan Y (2002). Temporal specificity in the cortical plasticity of visual space representation. *Science* **296**, 1999–2003.

Glazewski S & Fox K (1996). Time course of experience-dependent synaptic potentiation and depression in barrel cortex of adolescent rats. *J Neurophysiol* **75**, 1714–1729.

Glazewski S, Herman C, McKenna M, Chapman PF & Fox K (1998). Long-term potentiation in vivo in layers II/III of rat barrel cortex. *Neuropharmacology* **37**, 581–592.

Goldring S, Aras E & Weber PC (1970). Comparative study of sensory input to motor cortex in animals and man. *Electroencephalogr Clin Neurophysiol* **29**, 537–550.

Gow D, Hobson AR, Furlong P & Hamdy S (2004). Characterising the central mechanisms of sensory modulation in human swallowing motor cortex. *Clin Neurophysiol* **115**, 2382–2390.

Heusler P, Cebulla B, Boehmer G & Dinse HR (2000). A repetitive intracortical microstimulation pattern induces long-lasting synaptic depression in brain slices of the rat primary somatosensory cortex. *Exp Brain Res* **135**, 300–310.

Huang MX, Aine C, Davis L, Butman J, Christner R, Weisend M, Stephen J, Meyer J, Silveri J, Herman M & Lee RR (2000). Sources on the anterior and posterior banks of the central sulcus identified from magnetic somatosensory evoked responses using multistart spatio-temporal localization. *Hum Brain Mapp* **11**, 59–76.

Huang W, Armstrong-James M, Rema V, Diamond ME & Ebner FF (1998). Contribution of supragranular layers to sensory processing and plasticity in adult rat barrel cortex. *J Neurophysiol* **80**, 3261–3271.

Jones EG (1986). Connectivity of the primate sensory-motor cortex. In *Cerebral Cortex*, ed. Jones EG & Peters A, pp. 113–183. Plenum Press, New York.

Jones EG (2000). Cortical and subcortical contributions to activity-dependent plasticity in primate somatosensory cortex. *Annu Rev Neurosci* **23**, 1–37.

Kaas JH & Pons TP (1988). The somatosensory system in primates. *Comp Primate Biol* **4**, 421–468.

Keller A, Pavlides C & Asanuma H (1990). Long-term potentiation in the cat somatosensory cortex. *Neuroreport* **1**, 49–52.

Kitagawa H, Nishimura Y, Yoshioka K, Lin M & Yamamoto T (1997). Long-term potentiation and depression in layer III and V pyramidal neurons of the cat sensorimotor cortex in vitro. *Brain Res* **751**, 339–343.

Klem GH, Luders HO, Jasper HH & Elger C (1999). The ten-twenty electrode system of the International Federation. The International Federation of Clinical Neurophysiology. *Electroencephalogr Clin Neurophysiol Suppl* **52**, 3–6.

Knecht S, Henningsen H, Elbert T, Flor H, Hohling C, Pantev C & Taub E (1996). Reorganizational and perceptional changes after amputation. *Brain* **119**, 1213–1219.

Lee EK & Seyal M (1998). Generators of short latency human somatosensory-evoked potentials recorded over the spine and scalp. *J Clin Neurophysiol* **15**, 227–234.

Legatt AD & Kader A (2000). Topography of the initial cortical component of the median nerve somatosensory evoked potential. Relationship to central sulcus anatomy. *J Clin Neurophysiol* **17**, 321–325.

Lemon RN & van der Burg J (1979). Short-latency peripheral inputs to thalamic neurones projecting to the motor cortex in the monkey. *Exp Brain Res* **36**, 445–462.

Li C, Lu J, Wu C, Duan S & Poo M (2004). Bidirectional modification of presynaptic neuronal excitability accompanying spike timing-dependent synaptic plasticity. *Neuron* **41**, 257–268.

McLaughlin DF & Kelly EF (1993). Evoked potentials as indices of adaptation in the somatosensory system in humans: a review and prospectus. *Brain Res Brain Res Rev* **18**, 151–206.

Matsunaga K, Nitsche MA, Tsuji S & Rothwell JC (2004). Effect of transcranial DC sensorimotor cortex stimulation on somatosensory evoked potentials in humans. *Clin Neurophysiol* **115**, 456–460.

Mauguiere F, Allison T, Babiloni C, Buchner H, Eisen AA, Goodin DS, Jones SJ, Kakigi R, Matsuoka S, Nuwer M, Rossini PM & Shibasaki H (1999). Somatosensory evoked potentials. The International Federation of Clinical Neurophysiology. *Electroencephalogr Clin Neurophysiol Suppl* **52**, 79–90.

Merzenich MM, Kaas JH, Wall J, Nelson RJ, Sur M & Felleman D (1983). Topographic reorganization of somatosensory cortical areas 3b and 1 in adult monkeys following restricted deafferentation. *Neuroscience* **8**, 33–55.

Mitzdorf U (1985). Current source-density method and application in cat cerebral cortex: investigation of evoked potentials and EEG phenomena. *Physiol Rev* **65**, 37–100.

Moller AR, Jannetta PJ & Burgess JE (1986). Neural generators of the somatosensory evoked potentials: recording from the cuneate nucleus in man and monkeys. *Electroencephalogr Clin Neurophysiol* **65**, 241–248.

Nicholson Peterson N, Schroeder CE & Arezzo JC (1995). Neural generators of early cortical somatosensory evoked potentials in the awake monkey. *Electroencephalogr Clin Neurophysiol* **96**, 248–260.

Nicolelis MA, Katz D & Krupa DJ (1998). Potential circuit mechanisms underlying concurrent thalamic and cortical plasticity. *Rev Neurosci* **9**, 213–224.

Nuwer MR, Aminoff M, Desmedt J, Eisen AA, Goodin D, Matsuoka S, Mauguiere F, Shibasaki H, Sutherling W & Vibert JF (1994). IFCN recommended standards for short latency somatosensory evoked potentials. Report of an IFCN committee. International Federation of Clinical Neurophysiology. *Electroencephalogr Clin Neurophysiol* **91**, 6–11.

Okamoto M, Dan H, Sakamoto K, Takeo K, Shimizu K, Kohno S, Oda I, Isobe S, Suzuki T, Kohyama K & Dan I (2004). Three-dimensional probabilistic anatomical cranio-cerebral correlation via the international 10–20 system oriented for transcranial functional brain mapping. *Neuroimage* **21**, 99–111.

Pleger B, Dinse HR, Ragert P, Schwenkreis P, Malin JP & Tegenthoff M (2001). Shifts in cortical representations predict human discrimination improvement. *Proc Natl Acad Sci U S A* **98**, 12255–12260.

Pleger B, Foerster AF, Ragert P, Dinse HR, Schwenkreis P, Malin JP, Nicolas V & Tegenthoff M (2003). Functional imaging of perceptual learning in human primary and secondary somatosensory cortex. *Neuron* **40**, 643–653.

Pons TP, Garraghty PE, Ommaya AK, Kaas JH, Taub E & Mishkin M (1991). Massive cortical reorganization after sensory deafferentation in adult macaques. *Science* **252**, 1857–1860.

Ragert P, Becker M, Tegenthoff M, Pleger B & Dinse HR (2004). Sustained increase of somatosensory cortex excitability by 5 Hz repetitive transcranial magnetic stimulation studied by paired median nerve stimulation in humans. *Neurosci Lett* **356**, 91–94.

Regan D (1989). *Human Brain Electrophysiology: Evoked Potentials and Evoked Magnetic Fields in Science and Medicine*, chap. 1. Elsevier, New York.

Rossini PM, Barker AT, Berardelli A, Caramia MD, Caruso G, Cracco RQ, Dimitrijevic MR, Hallett M, Katayama Y, Lucking CH, Maertens de Noordhout AL, Marsden CD, Murray NMF, Rothwell JC, Swash M & Tomberg C (1994). Non-invasive electrical and magnetic stimulation of the brain, spinal cord and roots: basic principles and procedures for routine clinical application. Report of an IFCN committee. *Electroencephalogr Clin Neurophysiol* **91**, 79–92.

Rothwell JC (1997). Techniques and mechanisms of action of transcranial stimulation of the human motor cortex. *J Neurosci Meth* **74**, 113–122.

Sejnowski TJ (1999). The book of Hebb. *Neuron* **24**, 773–776.

Song S & Abbott LF (2001). Cortical development and remapping through spike timing-dependent plasticity. *Neuron* **32**, 339–350.

Song S, Miller KD & Abbott LF (2000). Competitive Hebbian learning through spike-timing-dependent synaptic plasticity. *Nat Neurosci* **3**, 919–926.

Sonoo M, Genba-Shimizu K, Mannen T & Shimizu T (1997). Detailed analysis of the latencies of median nerve somatosensory evoked potential components, 2: Analysis of subcomponents of the P13/14 and N20 potentials. *Electroencephalogr Clin Neurophysiol* **104**, 296–311.

Stefan K, Kunesch E, Benecke R, Cohen LG & Classen J (2002). Mechanisms of enhancement of human motor cortex excitability induced by interventional paired associative stimulation. *J Physiol* **543**, 699–708.

Stefan K, Kunesch E, Cohen LG, Benecke R & Classen J (2000). Induction of plasticity in the human motor cortex by paired associative stimulation. *Brain* **123**, 572–584.

Tinazzi M, Rosso T, Zanette G, Fiaschi A & Aglioti SM (2003). Rapid modulation of cortical proprioceptive activity induced by transient cutaneous deafferentation: neurophysiological evidence of short-term plasticity across different somatosensory modalities in humans. *Eur J Neurosci* **18**, 3053–3060.

Tinazzi M, Valeriani M, Moretto G, Rosso T, Nicolato A, Fiaschi A & Aglioti SM (2004). Plastic interactions between hand and face cortical representations in patients with trigeminal neuralgia: a somatosensory-evoked potentials study. *Neuroscience* **127**, 769–776.

Tinazzi M, Zanette G, La Porta F, Polo A, Volpato D, Fiaschi A & Mauguiere F (1997*a*). Selective gating of lower limb cortical somatosensory evoked potentials (SEPs) during passive and active foot movements. *Electroencephalogr Clin Neurophysiol* **104**, 312–321.

Tinazzi M, Zanette G, Polo A, Volpato D, Manganotti P, Bonato C, Testoni R & Fiaschi A (1997*b*). Transient deafferentation in humans induces rapid modulation of primary sensory cortex not associated with subcortical changes: a somatosensory evoked potential study. *Neurosci Lett* **223**, 21–24.

Tinazzi M, Zanette G, Volpato D, Testoni R, Bonato C, Manganotti P, Miniussi C & Fiaschi A (1998). Neurophysiological evidence of neuroplasticity at multiple levels of the somatosensory system in patients with carpal tunnel syndrome. *Brain* **121**, 1785–1794.

Tsuji T & Rothwell JC (2002). Long lasting effects of rTMS and associated peripheral sensory input on MEPs, SEPs and transcortical reflex excitability in humans. *J Physiol* **540**, 367–376.

Urban J, Kossut M & Hess G (2002). Long-term depression and long-term potentiation in horizontal connections of the barrel cortex. *Eur J Neurosci* **16**, 1772–1776.

Urbano A, Babiloni F, Babiloni C, Ambrosini A, Onorati P & Rossini PM (1997). Human short latency cortical responses to somatosensory stimulation. A high resolution EEG study. *Neuroreport* **8**, 3239–3243.

Vaughan JH & Arezzo J (1988). The neural basis of event-related potentials. In *Human Event-Related Potentials*, ed. Picton T, pp. 45–96. Elsevier, Amsterdam.

Werk CM & Chapman CA (2003). Long-term potentiation of polysynaptic responses in layer V of the sensorimotor cortex induced by theta-patterned tetanization in the awake rat. *Cereb Cortex* **13**, 500–507.

Wolters A, Sandbrink F, Schlottmann A, Kunesch E, Stefan K, Cohen LG, Benecke R & Classen J (2003). A temporally asymmetric Hebbian rule governing plasticity in the human motor cortex. *J Neurophysiol* **89**, 2339–2345.

Yamada T (2000). Neuroanatomic substrates of lower extremity somatosensory evoked potentials. *J Clin Neurophysiol* **17**, 269–279.

Yamada T, Matsubara M, Shiraishi G, Yeh M & Kawasaki M (1996). Topographic analyses of somatosensory evoked potentials following stimulation of tibial, sural and lateral femoral cutaneous nerves. *Electroencephalogr Clin Neurophysiol* **100**, 33–43.

Yao H & Dan Y (2001). Stimulus timing-dependent plasticity in cortical processing of orientation. *Neuron* **32**, 315–323.

Zhang W & Linden DJ (2003). The other side of the engram: experience-driven changes in neuronal intrinsic excitability. *Nat Rev Neurosci* **4**, 885–900.

Ziemann U, Iliac TV, Pauli C, Meintzschel F & Ruge D (2004). Learning modifies subsequent induction of long-term potentiation-like and long-term depression-like plasticity in human motor cortex. *J Neurosci* **24**, 1666–1672.

Ziemann U & Rothwell JC (2000). I-waves in motor cortex. *J Clin Neurophysiol* **17**, 397–405.

Acknowledgements

We acknowledge support from the Dystonia-Foundation, USA, and the State of Bavaria, Germany. We thank V. Litvak and S. Meuth for carefully reading the manuscript.